Scalar and anisotropic *J* interactions in undoped InP: A triple-resonance NMR study

Marco Tomaselli, David deGraw, Jeffery L. Yarger, Matthew P. Augustine,* and Alexander Pines
Materials Sciences Division, Lawrence Berkeley National Laboratory, Berkeley, California 94720
and Department of Chemistry, University of California, Berkeley, California 94720
(Received 6 April 1998)

The heteronuclear *J*-coupling tensor between nearest neighbor ^{31}P and ^{113}In spins in undoped InP is investigated by means of $^{113}\text{In}\rightarrow{}^{31}\text{P}$ polarization transfer under rapid magic angle spinning (MAS). The scalar contribution can be measured directly and is found to have the value $|J^{\text{iso}}(^{31}\text{P-}^{113,115}\text{In})|=(225\pm10)$ Hz. The principal value of the traceless anisotropic *J*-coupling tensor (pseudodipolar coupling) is determined to be $J^{\text{aniso}}(^{31}\text{P-}^{113,115}\text{In})=2/3[J_{\parallel}(^{31}\text{P-}^{113,115}\text{In})\text{-}J_{\perp}(^{31}\text{P-}^{113,115}\text{In})]=(813\pm50)$ or (1733 ± 50) Hz, assuming axial symmetry with the principal axis parallel to the In-P bond. Our values deviate from those reported previously [M. Engelsberg and R. E. Norberg, Phys. Rev. B **5**, 3395 (1972)] [based on a moment analysis of the ^{31}P resonance $|J^{\text{iso}}(^{31}\text{P-}^{113,115}\text{In})|=350$ Hz and $J^{\text{aniso}}(^{31}\text{P-}^{113,115}\text{In})=1273$ Hz], but confirm the postulate that the nearest neighbor $^{31}\text{P-}^{113,115}$In magnetic dipolar and pseudodipolar interactions are of the same order of magnitude and partially cancel each other. [S0163-1829(98)07137-9]

I. INTRODUCTION

It was recognized early that the electron-coupled nuclear-spin interactions (*J* coupling) in III-V binary semiconducting compounds with zinc-blende structure play a key role in the understanding of the experimentally observed nuclear magnetic resonance (NMR) spectra.[1–3] The accurate measurement of direct and indirect *J* couplings in bulk and nanostructured III-V compounds[4–8] is important in light of the determination of their electronic structures and can complement optical studies.[9,10]

InP is a prominent example where ''anomalous'' ^{31}P NMR linewidths have been observed and ascribed to the relative magnitudes of the direct heteronuclear anisotropic *J* coupling and the through-space dipole coupling. In their pioneering work, Engelsberg and Norberg[11] found that the dominant $^{31}\text{P-}^{113,115}$In contribution to the second moment of the ^{31}P resonance is a factor of 2 smaller than expected from the dipole-dipole interactions alone. Their finding was explained by a cancellation of the through-space dipole coupling between ^{31}P and ^{113,115}In by the anisotropic part of the direct neighbor $^{31}\text{P-}^{113,115}$In *J*-coupling tensor. More recently, Adolphi, Conradi, and Buhro[12] corroborated this assertion and obtained reasonable agreement with their experimental ^{31}P MAS spectrum, $\nu_{1/2}\sim4$ kHz, by calculating the nearest-neighbor scalar linewidth using Engelsberg and Norberg's result of $|J^{\text{iso}}(^{31}\text{P-}^{113,115}\text{In})|=350$ Hz.[11]

In contrast, Vanderah *et al.*[13] ascribed the observed ^{31}P MAS linewidth in InP, to quadrupolar effects of the neighboring ^{115}In spins. Indeed, Han *et al.*[14] observed spinning sidebands in the ^{113,115}In MAS spectra of InP. In their analysis, the broadening was attributed to small distributions of electric field gradients (EFG) causing some spreading of the satellite transition frequencies of ^{113,115}In at or near crystal defect sites.

In the present work, ^{31}P, ^{113}In, ^{115}In triple resonance combined with magic angle spinning is used to determine the dominant contributions to the ^{31}P linewidth. The heteronuclear *J*-coupling tensor between nearest-neighbor ^{31}P and ^{113}In spins in undoped InP is investigated by means of $^{113}\text{In}\rightarrow{}^{31}\text{P}$ polarization transfer under rapid magic angle spinning. Our results confirm that indium quadrupolar coupling constants in zinc-blende compounds are small and do not affect the observed NMR spectra, as previously predicted.[11,12,15] We confirm Engelsberg and Norberg's postulate that the ^{31}P NMR linewidth in InP is determined by the relative magnitude and sign of the direct heteronuclear anisotropic *J* coupling and the through-space dipole coupling.[11] The obtained values for $|J^{\text{iso}}(^{31}\text{P-}^{113,115}\text{In})|$ ($|J_{IS}^{\text{iso}}|$) and $J^{\text{aniso}}(^{31}\text{P-}^{113,115}\text{In})$ (J_{IS}^{aniso}), however, significantly deviate from previous results based on a moment analysis.[11,12]

II. EXPERIMENT

MAS experiments were performed on a InP single crystal of cylindrical shape (sample-1: 3 mm height; 2 mm diameter) with the [100] crystal axis inclined at the magic angle ($\Theta=54.74°$) with respect to the external magnetic field $\mathbf{B}_0$. The sample was machined from a large undoped [100] InP single crystal (99.999% purity; $N_D-N_A=5.7\times10^{15}$ cm^{-3}; $\mu_{300\,\text{K}}=3900$ cm^2/Vs) purchased from Crystallod Inc. Somerville, New York. A powder sample of the same material (sample-2) was prepared by grinding the above single crystal in a agate mortar. All MAS experiments were performed at ambient temperature on a Chemagnetics CMX spectrometer operating at a proton frequency of 400 MHz using a standard 4 mm MAS probe assembly from the same manufacturer [$\nu_0(^{31}\text{P})=161.196$ MHz, $\nu_0(^{115}\text{In})=87.753$ MHz, and $\nu_0(^{113}\text{In})=87.565$ MHz]. The MAS frequency was stabilized within 3 Hz for all experiments. Measurements with a static sample were performed on a home-built spectrometer operating at a proton frequency of 300 MHz [$\nu_0(^{31}\text{P})=121.93$ MHz, $\nu_0(^{115}\text{In})=66.055$ MHz] using a

home-built double-resonance probe assembly. Here, an undoped InP single crystal of rectangular shape (sample-3: 3 $\times 3 \times 1$ mm) was used to measure the anisotropy of the ^{31}P line shape. All ^{31}P ($I=1/2$) spectra were obtained by cross-polarization[16,17] from ^{115}In or ^{113}In (^{113,115}S$=9/2$). In both setups (MAS and static) the radio-frequency (rf) field strength on all channels (^{31}P, ^{115}In, and ^{113}In) was matched to 28 kHz. Numerical calculations for the MAS data were performed in the framework of the simulation environment GAMMA.[18]

The skin depth δ (Ref. 19) is estimated from the conductivity data of the InP material. For $\nu_0(^{31}\mathrm{P})=161.196$ MHz we obtain $\delta \sim 3$ mm, which is in the order of the dimension of the single crystal samples. Nonuniform penetration of the rf field into the InP samples (single crystals and powder) was not observed in our experiments.

III. NMR IN InP

A. ^{31}P line shape under MAS and ^{115}In decoupling

Figure 1 shows a set of ^{31}P spectra taken from the undoped InP powder sample. All spectra were obtained by a cross polarization[16,17] from the abundant ^{115}In spins (^{115}S$=$ 9/2; 95.72%) using a contact time[17] of $\tau_{cp}=0.5$ ms. The spectrum in Fig. 1(a) was recorded under static conditions with no ^{115}In decoupling during the acquisition time. Spectrum (b) was acquired under static conditions with ^{115}In decoupling using $\omega_{1S}/2\pi=60$ kHz. In both cases the line shape clearly deviates from a Gaussian and we characterize the spectra by numerically calculating the second moment (M_2)[19,20] of the ^{31}P resonance. We obtain a value of $\sqrt{M_2}/2\pi=2.74\pm0.2$ kHz for spectrum (a) and $\sqrt{M_2}/2\pi=0.60\pm0.1$ kHz for spectrum (b). Both values are in reasonable agreement with the ones given by Engelsberg and Norberg[11] and corroborate their finding that the undecoupled ^{31}P line shape [Fig. 1(a)] is dominated by ^{115}In-^{31}P couplings. The experimental second moment is about a factor of 2 smaller than expected from through-space dipole couplings alone.[11] The second moment obtained for spectrum (b) agrees with the calculated value of $\sqrt{M_2}/2\pi=0.70$ kHz based on through-space ^{31}P-^{31}P dipolar interactions alone.

It should be noted that the Hartmann-Hahn condition[16] for the cross polarization from ^{115}In (S) to ^{31}P (I) was matched at $\omega_{1S}=\omega_{1I}$ which is efficient when $|Q(^{115}\mathrm{In})| \ll \omega_{1S}$,[21] where Q denotes the first order quadrupole splitting. Hence, the spectra shown in Fig. 1 are representative for ^{31}P surrounded by ^{115}In with $Q\sim 0$, and quadrupole splitting effects due to potential crystal defects sites (i.e., dangling bonds on the surface, grain boundaries, bond strains, vacancies, substitutional defects) are suppressed. A series of ^{115}In nutation spectra[22] with 2 kHz$\leqslant \omega_{1S}/2\pi \leqslant$25 kHz (data not shown) recorded for the InP single crystal sample-3 additionally indicated that $|Q(^{115}\mathrm{In})|\sim 0$ throughout the crystal as expected for a cubic zinc-blende lattice.

Spectra (c) and (d) in Fig. 1 were obtained under rapid MAS conditions ($\omega_r/2\pi=10$ kHz) with additional on-resonance ^{115}In decoupling ($\omega_{1S}/2\pi=60$ kHz) during the acquisition period in (d). Identical spectra were obtained when the spinning speed was increased to $\omega_r/2\pi$

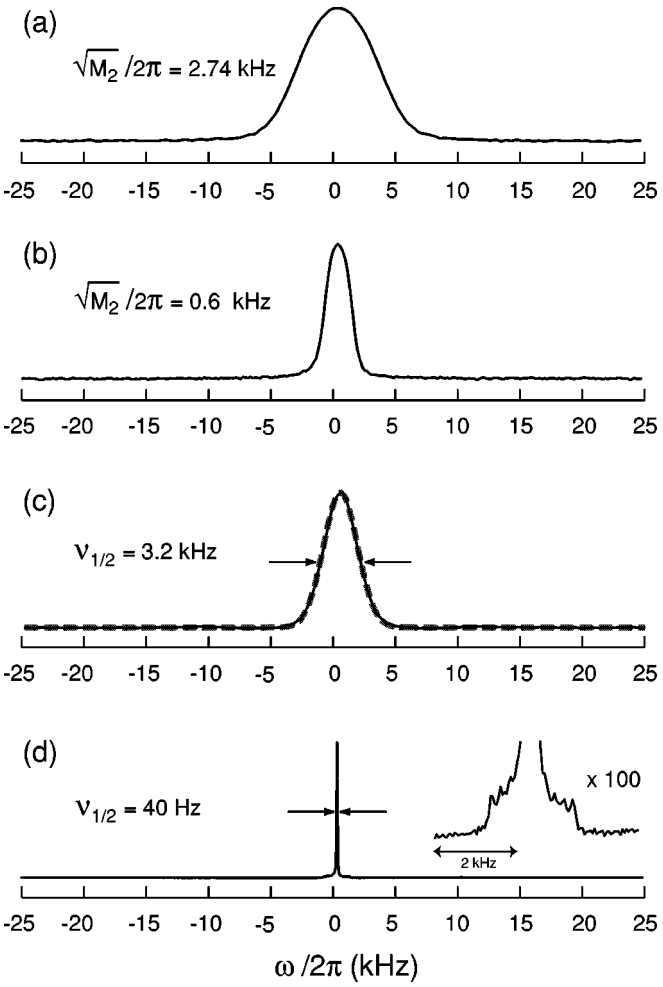

FIG. 1. ^{31}P spectra recorded for the undoped InP powder sample-2. All spectra were obtained by means of $^{115}\mathrm{In}\rightarrow{}^{31}\mathrm{P}$ cross polarization with a contact time of $\tau_{cp}=0.5$ ms. The radio-frequency amplitudes during τ_{cp} were matched to $\omega_{1S}/2\pi=\omega_{1I}/2\pi=28$ kHz. A total of 128 transients with a delay of 3 s was acquired for each spectrum. (a) A static spectrum without ^{115}In decoupling during the acquisition time. (b) Static with ^{115}In decoupling during the acquisition time ($\omega_{1S}/2\pi=60$ kHz). (c) MAS ($\omega_r/2\pi=10$ kHz), no ^{115}In decoupling during the acquisition time. (d) MAS ($\omega_r/2\pi=10$ kHz) with ^{115}In decoupling during the acquisition time ($\omega_{1S}/2\pi=60$ kHz). For spectra (a) and (b) the second moment (see text) was calculated according to $M_2=\int(\omega-\omega_0)^2 f(\omega)d\omega$, where $f(\omega)$ is the normalized experimental line shape function with a maximum at ω_0 (Ref. 19). A Gaussian fit (gray dashed line) is included for spectrum (c). The obtained values for M_2 and $\nu_{1/2}$ (full width at half height) are indicated in the figure. The ^{31}P satellite spectrum is shown in the inset of (d).

$=18$ kHz. Rapid magic angle spinning averages all interactions described by second rank tensors and thus, removes broadenings due to through-space dipolar, pseudodipolar and possible chemical shielding interactions affecting the ^{31}P line shape. The line shape is accurately described by a Gaussian in case (c). We obtain a full width at half height $\nu_{1/2}=2.36\sqrt{M_2}/2\pi=3.2\pm0.1$ kHz [see fit included in Fig. 1(c)]. Assuming that the second moment of spectrum (c) is determined by the local field of the 4 nearest ^{115}In neighbors[12,23] (caused by the scalar part of the ^{31}P-^{115}In J-coupling tensor) we estimate $|J_{IS}^{\mathrm{iso}}|=(250\pm50)$ Hz. The ob-

tained linewidth in spectrum (c) and therefore our estimate for $|J_{IS}^{\rm iso}|$ deviates from previous results where $\nu_{1/2}\sim 4$ kHz was reported.[12,13]

The narrow peak in spectrum (d) (MAS and ^{115}In on-resonance decoupling) is well described by a Lorentzian with $\nu_{1/2}=40$ Hz displaying only the isotropic part of the homonuclear ^{31}P interactions: the chemical shift is $\delta(\mathrm{In}^{31}\mathrm{P}) = -147$ ppm relative to the 85% H_3PO_4 standard.[24] The residual broadening in spectrum (d) is most likely due to bulk-susceptibility effects. The most interesting feature in (d), however, is the fine structure near the baseline of the spectrum shown in the inset of Fig. 1(d). This structure reveals the satellite spectrum of ^{31}P broadened by the local field of the rare ^{113}In spins (^{113}S=9/2; 4.28%). Assuming that the satellite spectrum is caused by the nearest neighbor ^{113}In spins the coupling Hamiltonian can be written as

$$H=H_{IS}+H_{II}=2\pi J_{IS}^{\rm iso}S_z\sum_{j=1}^{4} I_{jz}+2\pi J_{II}^{\rm iso}\sum_{j<k}^{4}\mathbf{I}_j\mathbf{I}_k . \quad (1)$$

Since $[H_{IS},H_{II}]=0$ and $[F_x,H_{II}]=0$, where $F_x=\Sigma_j^n I_{jx}$ denotes the detection operator, the homonuclear *I* spin scalar *J* couplings do not affect the spectrum. Thus the ^{31}P multiplet with a single ^{113}In neighbor consists of 10 lines of equal intensity, spaced by $J_{IS}^{\rm iso}$. Such a spectrum can indeed be observed for InP [see Fig. 2(a)] when a cross polarization from ^{113}In to ^{31}P is performed at the exact *centerband* Hartmann-Hahn condition[27–29] ($\omega_{1S}=\omega_{1I}$) under rapid MAS and ^{115}In decoupling during the acquisition period. The spectrum shown in Fig. 2(a) was recorded with $\omega_r/2\pi=10$ kHz and a contact time of $\tau_{cp}=0.8$ ms. An identical spectrum was obtained when the spinning speed was increased to $\omega_r/2\pi=18$ kHz. The details of the applied rf pulse sequence is displayed as an inset in Fig. 2(a). From the analysis of the multiplet in (a) we obtain for the nearest neighbor scalar *J* coupling $|J_{IS}^{\rm iso}|=(225\pm 10)$ Hz.[30] The value can be compared to our previous estimate of 250 ± 50 Hz based on spectrum (c) in Fig. 1 and to the value reported by others (350 Hz).[11,12] This demonstrates that isotropic *J* couplings obtained by a moment analysis of featureless static or MAS spectra[11,12,23] may deviate from the correct result by up to $\sim 50\%$.

Two additional features of the spectrum shown in Fig. 2(a) should be mentioned. First, a gradual decrease of the peak heights of the 10-line multiplet from the $\pm 9/2$ (outer) to the $\pm 1/2$ (inner) spin states of ^{113}In is observed. This can be explained by the longer lifetimes of the higher indium spin states. A similar trend has been observed by Wasylishen *et al.*[15] in a indium tribromid-triarylphosphine adduct compound. Second, the line in the center of the multiplet ($\sim 5\%$ of the total signal intensity) can be associated with the 36 next-nearest neighbor ^{31}P spins, weakly polarized by their nonvanishing scalar *J* couplings ($J_{IS}^{\rm iso'}$) to the ^{113}In.

B. ^{113}In→^{31}P polarization transfer under rapid magic angle spinning

For the spin system of one rare ^{113}In (*S*) spin and 4 nearest-neighbor ^{31}P (*I*) spins, the Hamiltonian active during the contact time of the cross-polarization experiment (see insets of Fig. 2), in the doubly rotating tilted frame,[31,32] with the *z* axis parallel to the rf irradiation, is approximated as

$$H=H_I+H_S+H_{IS,J^{\rm iso}}+H_{IS,b}(\tau). \quad (2)$$

Sufficiently strong resonant rf fields are assumed which lead to an efficient decoupling of the ^{115}In spins. Chemical shift terms are negligible in InP. Since $\omega_r \gg b_{II}^{jk}$, where b_{II}^{jk} denote the effective phosphorous dipolar coupling constants, we neglect the nonsecular homonuclear ^{31}P dipolar interaction $H_{II,b}$. The interactions with the rf fields are given by $H_I=\omega_{1I}F_z$ and $H_S=\omega_{1S}S_z$. Dropping nonsecular terms with

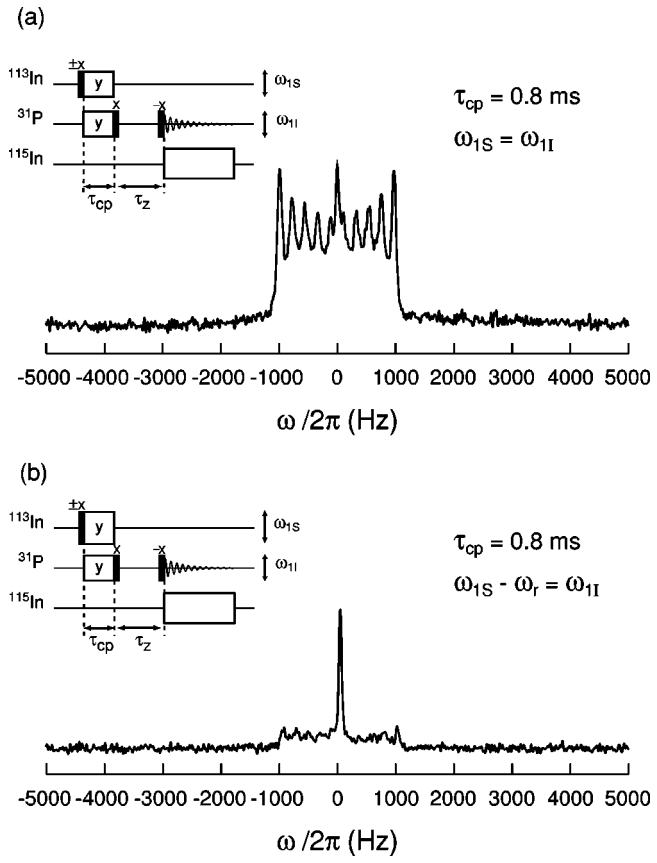

FIG. 2. MAS ^{31}P spectra obtained from the undoped InP powder sample-2. The spectra were obtained by means of ^{113}In→^{31}P cross polarization with a contact time of $\tau_{cp}=0.8$ ms and $\omega_r/2\pi=10$ kHz. In both cases, ^{115}In decoupling with $\omega_{1S}/2\pi=60$ kHz was applied during the acquisition period. The details of the radio-frequency pulse sequences are schematically drawn as insets in (a) and (b). The black boxes denote 90° pulses. In both cases a short *z*-filter period (Ref. 25) ($\tau_z=0.5$ ms) is used to guarantee pure phase spectra (Ref. 26). A total of 512 transients with a delay of 3 s was acquired for both experiments. In (a) the rf amplitudes during τ_{cp} were matched at the exact centerband Hartmann-Hahn condition (*J* cross polarization) (Refs. 27–29): $\omega_{1S}/2\pi=\omega_{1I}/2\pi=28$ kHz In (b) the rf amplitudes were exactly matched at the +1 Hartmann-Hahn sideband condition (Refs. 27–29): $(\omega_{1I}+\omega_r)/2\pi=\omega_{1S}/2\pi=38$ kHz. The observed splitting between each of the 10 multiplet peaks is the same within the experimental resolution (i.e., 225 ± 10 Hz). Based on a numerical simulation of the ^{31}P-^{113}In *J* coupling pattern we concluded that the effect of ^{115}In decoupling during the acquisition period with $\omega_{1S}/2\pi=60$ kHz has negligible effect on the separation of the ^{31}P multiplet lines.

respect to the truncation of the strong radio frequency fields, the heteronuclear scalar coupling interaction (time independent) is given by

$$H_{IS,J^{\rm iso}}=\frac{\pi}{2}J_{IS}^{\rm iso}\sum_{j=1}^{4}(I_j^+S^-+I_j^-S^+). \tag{3}$$

MAS renders the through space dipolar and anisotropic J interactions time dependent:

$$H_{IS,b}(\tau)=\frac{1}{2}\sum_{j=1}^{4}\sum_{n=-2}^{2}b_n^j e^{in\omega_r\tau}(I_j^+S^-+I_j^-S^+) \tag{4}$$

with the Fourier coefficients

$$b_0^j=0,\ b_{\pm1}^j=-\frac{1}{2\sqrt{2}}(d_{IS}+\pi J_{IS}^{\rm aniso})\sin(2\Theta_j)e^{\pm i\varphi_j}, \tag{5}$$

$$b_{\pm2}^j=\frac{1}{4}(d_{IS}+\pi J_{IS}^{\rm aniso})\sin^2(\Theta_j)e^{\pm2i\varphi_j}.$$

The heteronuclear through-space dipolar coupling constant is given in units of angular frequency as $d_{IS}=-\mu_0\gamma_I\gamma_S\hbar/4\pi r_{IS}^3$. In the zinc-blende structure of InP with a lattice constant of $a=5.87$ Å at 300 K (Ref. 33) we extract $d_{IS}/2\pi=-637$ Hz for the nearest neighbor ^{113}In-^{31}P pairs. $J_{IS}^{\rm aniso}$ denotes the principal value of the traceless anisotropic J-coupling tensor (pseudodipolar coupling). The polar angles Θ_j and φ_j describe the direction of the internuclear vectors $\mathbf{r}_{IS,j}$ with respect to the MAS rotor-fixed coordinate system with its z axis along the spinning axis. For the InP single crystal sample-1 with the [100] crystal axis along the rotor axis $\Theta_j=\Theta=54.74°$ (local tetrahedral symmetry) and φ_j can be set to zero.

It should also be mentioned that in Eqs. (4) and (5) we have implicitly assumed that the ^{113}In-^{31}P J-coupling tensor is axially symmetric with its principal axis parallel to the bond (colinear with the through-space dipole coupling tensor). This assumption is well supported by the threefold axis of symmetry along all nearest neighbor In-P bonds (space group $F\bar{4}3m$). We briefly summarize the two cases that lead to efficient cross polarization in InP:

(i) J cross polarization at the centerband Hartmann-Hahn condition[26,34,35] $\omega_{1S}=\omega_{1I}=\omega_1$. Here, $H_{IS,b}(\tau)$ can be neglected as nonsecular and Eq. (2) is simplified to

$$H_J^{cp}=\omega_1(S_z+F_z)+\frac{\pi}{2}J_{IS}^{\rm iso}\sum_{j=1}^{4}(I_j^+S^-+I_j^-S^+). \tag{6}$$

^{113}In$\rightarrow^{31}$P MAS J cross polarization in InP is well described by the Hamiltonian of Eq. (6). A representative spectrum is shown in Fig. 2(a) and was discussed in Sec. A.

(ii) Cross polarization at the ''sidebands'' of the Hartmann-Hahn condition $\omega_{1S}-\omega_{1I}=m\omega_r$ with $m=\pm1$, ±2. In this case, the Hamiltonian of Eq. (2) can be approximated by[27,29]

$$\bar{H}_{b,m}^{cp}=(\omega_{1S}-m\omega_r)S_z+\omega_{1I}F_z+H_{IS,m}, \tag{7}$$

with

$$H_{IS,\pm1}=-\frac{1}{2\sqrt{2}}(d_{IS}+\pi J_{IS}^{\rm aniso})\times\sum_{j=1}^{4}\sin(2\Theta_j)\tfrac{1}{2}(I_j^+S^-e^{\pm i\varphi_j}+I_j^-S^+e^{\mp i\varphi_j}) \tag{8}$$

and

$$H_{IS,\pm2}=\tfrac{1}{4}(d_{IS}+\pi J_{IS}^{\rm aniso})\times\sum_{j=1}^{4}\sin^2(\Theta_j)\tfrac{1}{2}(I_j^+S^-e^{\pm2i\varphi_j}+I_j^-S^+e^{\mp2i\varphi_j}). \tag{9}$$

In both cases (i) and (ii), the observed signal intensity of the 10-line multiplet can be calculated according to

$$\langle F_z(\tau_{cp})\rangle={\rm Tr}\{F_z e^{-iH_\alpha^{cp}\tau_{cp}}S_z e^{iH_\alpha^{cp}\tau_{cp}}\}, \tag{10}$$

where $\alpha=J$ or b,m. Analytical solutions of Eq. (10) can be found in the literature.[34]

A representative ^{31}P spectrum obtained by an ^{113}In $\rightarrow^{31}$P cross-polarization experiment at the $+1$-sideband condition ($\tau_{cp}=0.8$ ms, $\omega_r/2\pi=10$ kHz, $\omega_{1I}=\omega_{1S}-\omega_r$) is shown in Fig. 2(b). Here, the polarization transfer to the nearest neighbor I spins is exclusively driven by the ''effective'' dipolar coupling constant

$$b_{IS}^{\rm eff}=d_{IS}+\pi J_{IS}^{\rm aniso}, \tag{11}$$

and provides the possibility to measure $J_{IS}^{\rm aniso}$ selectively. This is in contrast to the centerband cross-polarization condition, where the polarization transfer is mediated through $J_{IS}^{\rm iso}$. The observed multiplet in Fig. 2(b) (45% of the total signal intensity) indicates that $d_{IS}+\pi J_{IS}^{\rm aniso}\neq0$, and the assumption of a fortuitous cancellation of d_{IS} and $\pi J_{IS}^{\rm aniso}$ (Ref. 11) is not confirmed. The much larger relative intensity of the central peak in Fig. 2(b) compared to the spectrum obtained under J cross-polarization conditions [Fig. 2(a)] indicates an efficient polarization transfer to more remote ^{31}P spins at the $+1$-sideband cross-polarization matching condition.

The buildup of the total signal intensity as a function of τ_{cp} is shown in Fig. 3(a) for the InP single crystal sample-1 ($\omega_r/2\pi=10$ kHz). The J cross-polarization transfer curve (circles) shows the well known transient oscillations[36] characteristic of isolated spin systems (I_4S in the case of InP). The solid line represents a calculated curve based on Eqs. (6) and (11) with $|J_{IS}^{\rm iso}|=225$ Hz and taking into account $T_{1\rho}(^{113}{\rm In})=30$ ms.[37] The first maximum of the experimental transient oscillations was normalized to the predicted value. As expected, the experimental oscillations deviate for long contact times caused by residual rf inhomogeneities. However, the agreement between the calculation and the experimental curve is satisfactory.

On the other hand, the transfer curve at the $+1$-sideband matching condition (crosses) is characteristic for an open spin system due to the extended network of ^{31}P nuclei, through-space dipole coupled to the dilute indium-113. Obviously, the Hamiltonian of Eqs. (8) and (9) cannot explain this transfer curve and the contribution from polarized re-

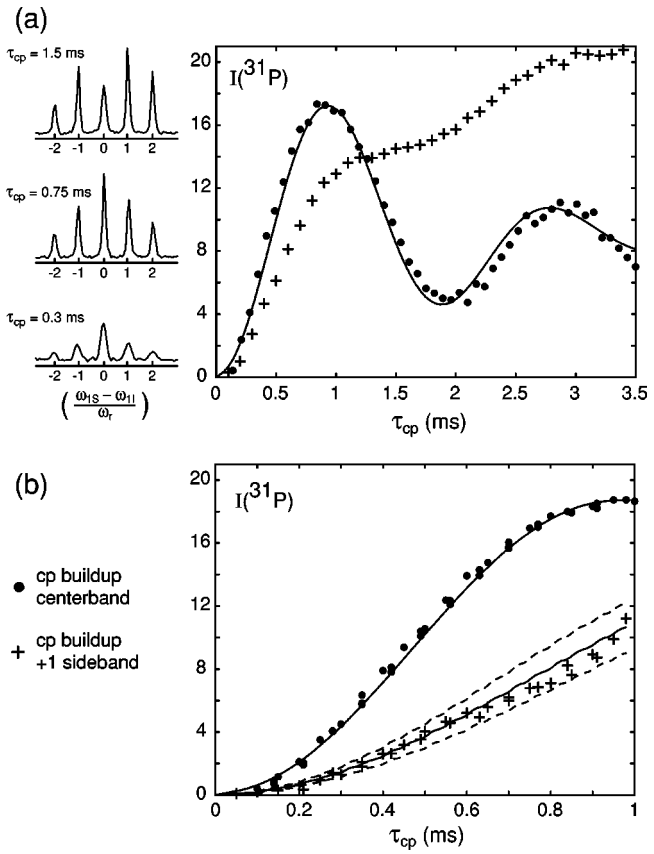

FIG. 3. (a) Total intensity of the ^{31}P resonance (^{113}In→^{31}P polarization transfer) in the InP single crystal sample-1 as a function of the contact time τ_{cp} under *J* cross-polarization conditions (circles) with $\omega_{1S}/2\pi=\omega_{1I}/2\pi=28$ kHz and for the +1-sideband matching condition (crosses) with $(\omega_{1I}+\omega_r)/2\pi=\omega_{1S}/2\pi=38$ kHz. The thin line denotes the calculation with $|J_{IS}^{\rm iso}|=225$ Hz. Also shown are typical experimental MAS cross polarization matching profiles for sample-1 at $\tau_{cp}=0.3$, 0.75, and 1.5 ms. Here, the ^{31}P rf amplitude was fixed at 28 kHz and the ^{113}In amplitude was varied between 0 and 60 kHz. The width of the center and sidebands are all equal for a given τ_{cp} and possibly caused by small residual rf inhomogeneities. (b) Buildup of the ^{31}P multiplet intensity (^{113}In→^{31}P polarization transfer) in the InP single crystal sample-1 for $0\leqslant\tau_{cp}\leqslant 1$ ms under *J* cross-polarization conditions (circles) with $\omega_{1S}/2\pi=\omega_{1I}/2\pi=28$ kHz and for the +1-sideband matching condition (crosses) with $(\omega_{1I}+\omega_r)/2\pi=\omega_{1S}/2\pi=38$ kHz. The full lines denote the theoretical prediction with $|J_{IS}^{\rm iso}|=225$ Hz (centerband) and a fit with $|b_{IS}^{\rm eff}|/2\pi=230\pm25$ Hz (+1-sideband). The dashed lines denote the calculated buildup for $|b_{IS}^{\rm eff}|/2\pi=255$ Hz and $|b_{IS}^{\rm eff}|/2\pi=205$ Hz, respectively. Experimental data were acquired with a spinning speed of $\omega_r/2\pi=10$ kHz. A total of 256 transients with a delay of 3 s was acquired for each data point. The normalization of the experimental data is described in the text. The intensity scale is given in units of the equilibrium polarization of one ^{31}P spin.

mote ^{31}P spins [central peak in Fig. 2(b)] has to be subtracted in order to extract $|b_{IS}^{\rm eff}|$. This is shown in Fig. 3(b) for $0\leqslant\tau_{cp}\leqslant 1$ ms, where damping effects due to $T_{1\rho}$(^{113}In) relaxation and rf inhomogeneities are negligible. The intensity of the 10-line multiplet was obtained by fitting the central line using a Lorentzian and subtracting its intensity from the total. The obtained experimental transfer curve is plotted in Fig. 3(b) (crosses) together with a fitted curve [Eqs. (8) and (10)] using the known orientation of the [100] crystal axis of sample-1 with respect to the static magnetic field ($\Theta=54.74°$). Both curves (experimental and fit) are normalized with respect to the first maximum of the transient oscillations observed under *J* cross-polarization conditions [displayed in Fig. 3(b) for comparison]. From the least-squares fit we obtain $|b_{IS}^{\rm eff}/2\pi|=|d_{IS}/2\pi+1/2J_{IS}^{\rm aniso}|=(230\pm25)$ Hz. This leads to the principal value of the nearest neighbor *J*-coupling tensor $J_{IS}^{\rm aniso}=(813\pm50)$ Hz or (1733 ± 50) Hz.[38]

C. Static orientation-dependent ^{31}P line shape

The values obtained for $J_{IS}^{\rm aniso}$ suggests that a considerable anisotropy for the second moment of the ^{31}P resonance should be expected for a static single crystal sample. Since the result of $J_{IS}^{\rm aniso}\sim1270$ Hz (Ref. 11) was mainly based on the lack of any modulation of M_2 as a function of the InP single crystal orientation with respect to $\mathbf{B}_0$, we repeated the static measurements for three different sets of orientations. The static experiments additionally provide an independent comparison to the experiments performed under MAS. Rotation patterns were obtained for the single crystal sample-3 with three different rotation axes **R**: (i) **R** parallel to [100], (ii) **R** parallel to [110], and in (iii) $\angle(\mathbf{R},[100])=45°$. In all cases the rotation axis was perpendicular to $\mathbf{B}_0$. All ^{31}P spectra were obtained by a cross polarization from the abundant ^{115}In spins with $\tau_{cp}=1$ ms. No ^{115}In decoupling was applied during the acquisition time.

The dominant part of the Hamiltonian determining the second moment of the static ^{115}In-coupled ^{31}P line shape can be approximated as (in the doubly rotating frame)

$$H=H_{II,d}+H_{IS}^{\rm near}+H_{IS}^{\rm far}, \tag{12}$$

with

$$H_{II,d}=\sum_{j<k} d_{II}^{jk}P_2(\cos\,\vartheta_{jk})(3I_{jz}I_{kz}-\mathbf{I}_j\mathbf{I}_k), \tag{13}$$

$$H_{IS}^{\rm near}=\sum_{j,k_j}[\pi J_{IS}^{\rm iso}+b_{IS}^{\rm eff}P_2(\cos\,\vartheta_{jk_j})]2I_{jz}S_{k_jz}, \tag{14}$$

and

$$H_{IS}^{\rm far}=\sum_{j,I\neq k_j} d_{IS}^{jI}P_2(\cos\,\vartheta_{jI})2I_{jz}S_{Iz}, \tag{15}$$

where $P_2(\cos\vartheta)$ is the normalized second-order Legendre polynomial,[39] and ϑ denotes the inclination angle of the internuclear vector with the external static magnetic field. Electron-coupled ^{31}P-^{31}P *J* interactions are neglected in Eqs. (12) and (13). Further, we have only included the *J*-coupling interactions between the nearest neighbor ^{115}In-^{31}P pairs in Eqs. (14) and (15). From Eqs. (12)–(15) we obtain the following expression for the second moment:[19,20]

$$M_2=M_2^{II,d}+M_2^{IS,\rm near}+M_2^{IS,\rm far}, \tag{16}$$

with the ^{31}P homonuclear through-space dipolar contribution

$$M_2^{II,d}=3I(I+1)\sum_k[d_{II}^{jk}P_2(\cos\,\vartheta_{jk})]^2, \tag{17}$$

the nearest-neighbor ^{115}In-^{31}P heteronuclear contribution

$$M_2^{IS,\mathrm{near}} = \frac{4}{3}S(S+1)(\pi J_{IS}^{\mathrm{iso}})^2 + \frac{16}{3}S(S+1)(b_{IS}^{\mathrm{eff}})^2\sum_{k_j}^{4}[P_2(\cos\vartheta_{jk_j})]^2 + \frac{16}{3}S(S+1)b_{IS}^{\mathrm{eff}}\pi J_{IS}^{\mathrm{iso}}\sum_{k_j}^{4}P_2(\cos\vartheta_{jk_j}), \tag{18}$$

and the heteronuclear through-space dipolar contribution

$$M_2^{IS,\mathrm{far}} = \tfrac{4}{3}S(S+1)\sum_{l\neq k_j}[d_{IS}^{jl}P_2(\cos\vartheta_{jl})]^2. \tag{19}$$

Note that, in principle, the last term of Eq. (18) provides the possibility to extract the relative sign of J_{IS}^{iso} and b_{IS}^{eff}, and therefore, to uniquely determine J_{IS}^{aniso}.[40] However, in the InP zinc-blende structure with its local tetrahedral symmetry, $\Sigma P_2(\cos\vartheta_{jk_j})=0$, and the ''cross term'' between J_{IS}^{iso} and b_{IS}^{eff} does not contribute to the total second moment.

Figure 4 shows the experimental rotation patterns of $\sqrt{M_2}$ for sample-3 and the three different single crystal orientations described above. Also included in Fig. 4 is a fit of $\sqrt{M_2}$ based on Eqs. (16)–(19) and using the known crystal structure of InP.[33] The lattice sums involved in the calculation of M_2 [Eqs. (17) and (19)] were evaluated by adding the contributions from 64 unit cells. $|J_{IS}^{\mathrm{iso}}|$ was constrained within 225 ± 10 Hz and $|b_{IS}^{\mathrm{eff}}|$ left unconstrained for the simultaneous fit of the three rotation patterns. Considering the rather crude approximations made in Eqs. (12)–(19) for the evaluation of the theoretical second moment, the fit is satisfactory, and we obtain $|b_{IS}^{\mathrm{eff}}/2\pi| = (245\pm80)$ Hz, in agreement with the value obtained under MAS conditions.

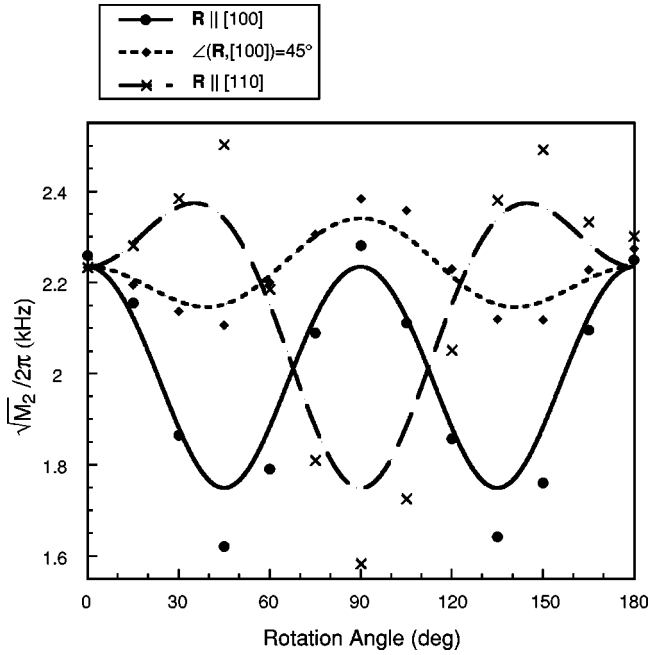

FIG. 4. Variation of $\sqrt{M_2}/2\pi$ of the static ^{31}P resonance as a function of the orientation of the InP single crystal sample-3 with respect to the external magnetic field: (i) **R** parallel to [100], (ii) **R** parallel to [110], (iii) $\angle(\mathbf{R},[100])=45°$. All ^{31}P spectra were obtained by a cross polarization from the abundant ^{115}In spins with $\tau_{cp}=1$ ms ($\omega_{1S}/2\pi=\omega_{1I}/2\pi=28$ kHz). The crystal rotation axis **R** was always perpendicular to $\mathbf{B}_0$. The experimental values of M_2 were numerically calculated from the ^{31}P spectra (see caption of Fig. 1). A total of 64 transients with a delay of 2 s was acquired for each orientation. Symbols indicate the experimental data, while the lines denote the result of a simultaneous least-squares fit of the three rotation patterns with $|J_{IS}^{\mathrm{iso}}|$ constrained within 225 ± 10 Hz and $|b_{IS}^{\mathrm{eff}}|$ left unconstrained. Note that the InP crystal orientation with the smallest modulation in the $\sqrt{M_2}/2\pi$ rotation pattern (i.e., $\angle(\mathbf{R},[100])=45°$) is identical to the one investigated by Engelsberg and Norberg (Ref. 11).

IV. SUMMARY

The combination of cross polarization and rapid magic angle spinning has proved useful in the measurement of scalar and anisotropic J interactions in the InP semiconductor. We confirmed the assertion of Engelsberg and Norberg that the ^{31}P NMR linewidth in undoped InP is determined by the relative magnitude and sign of the nearest-neighbor heteronuclear anisotropic J coupling (pseudodipolar) and through-space dipolar coupling.[11] We obtain by an independent set of experiments $|J^{\mathrm{iso}}(^{31}\mathrm{P}\text{-}^{113,115}\mathrm{In})| = (225\pm10)$ Hz for the scalar and $J^{\mathrm{aniso}}(^{31}\mathrm{P}\text{-}^{113,115}\mathrm{In}) = 2/3[J_{\parallel}(^{31}\mathrm{P}\text{-}^{113,115}\mathrm{In})\text{-}J_{\perp}(^{31}\mathrm{P}\text{-}^{113,115}\mathrm{In})] = (813\pm50)$ Hz or (1733 ± 50) Hz for the pseudodipolar contribution, respectively. The relative sign of $J^{\mathrm{iso}}(^{31}\mathrm{P}\text{-}^{113,115}\mathrm{In})$ and $b^{\mathrm{eff}}(^{31}\mathrm{P}\text{-}^{113,115}\mathrm{In})$ could not be determined in this study and results in an ambiguity in the anisotropic J coupling.

The large anisotropic $\mathbf{J}(^{31}\mathrm{P}\text{-}^{113,115}\mathrm{In})$ tensor emphasizes the importance of spin-spin coupling mechanisms other than the Fermi-contact mechanism in InP. In particular, the ratio $\frac{1}{2}|J^{\mathrm{aniso}}/J^{\mathrm{iso}}| = 1.80$ (Refs. 11,41) or 3.85 implies a predominantly p character of the In-P electronic wave function. The obtained values corroborate the interpretation of Engelsberg and Norberg that the large anisotropy of $\mathbf{J}(^{31}\mathrm{P}\text{-}^{113,115}\mathrm{In})$ is probably due to the proximity of the second lowest conduction band (p-like) and the first conduction band along [100] crystal directions.[10,42]

It should also be mentioned that the smaller of the two possible values of $J^{\mathrm{aniso}}(^{31}\mathrm{P}\text{-}^{113,115}\mathrm{In})$ in InP coincides with the only other reliable measurement of an In-P pseudodipolar coupling constant.[15] In addition, the corresponding ratio for $\frac{1}{2}|J^{\mathrm{aniso}}/J^{\mathrm{iso}}|$ is identical to the one estimated by Engelsberg and Norberg.

The experiments described above represent an initial application of double and triple resonance MAS NMR to the quantification of isotropic and anisotropic J couplings in a bulk III-V semiconductor. InP is a particularly well-suited material due to the low natural abundance of ^{113}In and the vanishing indium quadrupole coupling constant in a zinc-blende lattice. Similar experiments may also be useful in the study of electron-coupled nuclear spin interactions in II-VI semiconductors, semiconductor alloys,[4,5,43] or semiconductor nanocrystals.[6,7,44,45]

ACKNOWLEDGMENTS

We thank Dr. G. C. Chingas for helpful discussions and R. H. Havlin for providing the single crystal sample used for

the MAS experiments. This work was supported by the Director, Office of Energy Research, Office of Basic Energy Sciences, Materials Sciences Division, U.S. Department of Energy, under Contract No. DE-AC03-76SF00098. J.L.Y. and M.P.A. thank the support of the National Science Foundation under Grant No. DGE-9714523 and Grant No. CHE-9504655, respectively. M.T. acknowledges support from the Swiss National Foundation of Science.

*Present address: Department of Chemistry, University of California, Davis, CA 95616.

[1] M. A. Ruderman and C. Kittel, Phys. Rev. **96**, 99 (1954).

[2] N. Bloembergen and T. J. Rowland, Phys. Rev. **97**, 1679 (1955).

[3] P. W. Anderson, Phys. Rev. **99**, 623 (1955).

[4] T. M. Duncan, R. F. Karlicek, Jr., W. A. Bonner, and F. A. Thiel, J. Phys. Chem. Solids **45**, 389 (1984).

[5] R. Tycko, G. Dabbagh, S. R. Kurtz, and J. P. Goral, Phys. Rev. B **45**, 13 452 (1992).

[6] L. E. Brus, J. Phys. Chem. **90**, 2555 (1986).

[7] A. A. Guzelian, J. E. B. Katari, A. V. Kadavanich, U. Banin, K. Hamad, E. Juban, P. Alivisatos, R. H. Wolters, C. C. Arnold, and J. R. Heath, J. Phys. Chem. **100**, 7212 (1996).

[8] H. Fu and A. Zunger, Phys. Rev. B **56**, 1496 (1997).

[9] C. F. Klingshirn, *Semiconductor Optics* (Springer, Berlin, 1997).

[10] P. Y. Yu and M. Cardona, *Fundamentals of Semiconductors* (Springer, Berlin, 1996).

[11] M. Engelsberg and R. E. Norberg, Phys. Rev. B **5**, 3395 (1972).

[12] N. Adolphi, M. S. Conradi, and W. E. Buhro, J. Phys. Chem. Solids **53**, 1073 (1992).

[13] T. A. Vanderah and R. A. Nissan, J. Phys. Chem. Solids **49**, 1335 (1988).

[14] O-H. Han, H-K. C. Timken, and E. Oldfield, J. Chem. Phys. **89**, 6046 (1988).

[15] R. E. Wasylishen, K. C. Wright, K. Eichele, and T. S. Cameron, Inorg. Chem. **33**, 407 (1993).

[16] S. R. Hartmann and E. L. Hahn, Phys. Rev. **128**, 2024 (1962).

[17] A. Pines, M. G. Gibby, and J. S. Waugh, J. Chem. Phys. **59**, 569 (1973).

[18] S. A. Smith, T. O. Levante, B. H. Meier, and R. R. Ernst, J. Magn. Reson., Ser. A **106**, 75 (1994).

[19] A. Abragam, *Principles of Nuclear Magnetism* (Clarendon, Oxford, 1961).

[20] C. P. Slichter, *Principles of Magnetic Resonance* (Springer, Berlin, 1989).

[21] A. Vega, Solid State Nucl. Magn. Reson. **1**, 17 (1992).

[22] A. P. M. Kentgens, Ph.D. thesis, University of Nijmegen, 1987.

[23] L. D. Potter and Y. Wu, J. Magn. Reson., Ser. A **116**, 107 (1995).

[24] T. M. Duncan, *A Compilation of Chemical Shift Anisotropies* (Fargut Press, Chicago, 1990).

[25] R. R. Ernst, G. Bodenhausen, and A. Wokaun, *Principles of Nuclear Magnetic Resonance in One and Two Dimensions* (Clarendon, Oxford, 1987).

[26] A. Verhoeven, R. Verel, and B. H. Meier, Chem. Phys. Lett. **266**, 465 (1997).

[27] S. Hediger, B. H. Meier, and R. R. Ernst, J. Chem. Phys. **102**, 4000 (1995).

[28] D. Marks and S. Vega, J. Magn. Reson., Ser. A **118**, 157 (1996).

[29] B. H. Meier, Chem. Phys. Lett. **188**, 201 (1992).

[30] The scalar indirect spin-spin coupling constant can be written as $J^{\mathrm{iso}}(^{31}\mathrm{P}\text{-}^{\alpha}\mathrm{In}) = \hbar/2\pi\gamma_{\alpha_{\mathrm{In}}}\gamma_{^{31}\mathrm{P}}\mathrm{K(In,P)}$, where $\alpha = 113,115$ and K(In,P) denotes the reduced coupling constant (Ref. 3), which depends on the electronic properties and the internuclear distance. Since $\gamma_{^{113}\mathrm{In}}/\gamma_{^{115}\mathrm{In}} = 0.9979$ isotope effects on $J^{\mathrm{iso}}(^{31}\mathrm{P}\text{-}^{113,115}\mathrm{In})$ are small and within our experimental error.

[31] M. Mehring, *High Resolution NMR in Solids* (Springer, Berlin, 1983).

[32] U. Haeberlen, *Advances in Magnetic Resonance, Suppl. 1 High Resolution NMR in Solids* (Academic, New York, 1976).

[33] G. Gieske and H. Pfister, Acta Crystallogr. **11**, 369 (1958).

[34] L. Müller and R. R. Ernst, Mol. Phys. **38**, 963 (1979).

[35] R. D. Bertrand, W. B. Monitz, A. N. Garroway, and G. C. Chingas, J. Am. Chem. Soc. **100**, 5227 (1978); G. C. Chingas, A. N. Garroway, R. D. Bertrand, and W. B. Monitz, J. Chem. Phys. **74**, 127 (1981).

[36] L. Müller, A. Kumar, T. Baumann, and R. R. Ernst, Phys. Rev. Lett. **32**, 1402 (1974).

[37] The value $T_{1\rho}(^{113}\mathrm{In}) = 30$ ms was measured separately under the same experimental conditions as in the cross-polarization experiments; $\omega_r/2\pi = 10$ kHz and $\omega_{1S}/2\pi = 28$ kHz. $T_{1\rho}(^{31}\mathrm{P}) > 80$ ms for our experimental conditions and does not affect the polarization transfer curves.

[38] Due to our definition of the through-space dipolar coupling constant as $d_{IS}^{jk} = -\mu_0\gamma_I\gamma_S\hbar/4\pi r_{jk}^3$ the sign of J_{IS}^{aniso} is positive. This is in contrast to the convention used by Engelsberg and Norberg (Ref. 11).

[39] D. M. Brink and G. R. Satchler, *Angular Momentum* (Clarendon, Oxford, 1994).

[40] The relative sign of J_{IS}^{iso} and b_{IS}^{eff} can be determined only in special cases. Examples are given by Wasylishen *et al.* (Ref. 15) or by A. Nolle, Z. Phys. B **34**, 175 (1979).

[41] S. Clough and W. I. Goldburg, J. Chem. Phys. **45**, 4080 (1966).

[42] *Numerical Data and Functional Relationships in Science and Technology*, edited by K. H. Hellwege, Landolt-Börnstein, New Series, Group III, Vol. 17, Pt. b (Springer, Berlin, 1982).

[43] D. B. Zax, D. Zamir, and S. Vega, Phys. Rev. B **47**, 6304 (1993).

[44] A. M. Thayer, M. L. Steigerwald, T. M. Duncan, and D. C. Douglass, Phys. Rev. Lett. **60**, 2673 (1988).

[45] L. R. Becerra, C. B. Murray, R. G. Griffin, and M. G. Bawendi, J. Chem. Phys. **100**, 3297 (1994).